PHYSICAL REVIEW A **88**, 043637 (2013)

Optical tweezers for vortex rings in Bose-Einstein condensates

A. I. Yakimenko,[1] Yu. M. Bidasyuk,[2] O. O. Prikhodko,[1] S. I. Vilchinskii,[1] E. A. Ostrovskaya,[3] and Yu. S. Kivshar[3]
[1]*Department of Physics, Taras Shevchenko National University, Kyiv 01601, Ukraine*
[2]*Bogoliubov Institute for Theoretical Physics, National Academy of Ukraine, Kyiv 03680, Ukraine*
[3]*Nonlinear Physics Centre, Research School of Physics and Engineering, Australian National University, Canberra ACT 0200, Australia*
(Received 9 August 2013; published 28 October 2013)

We study generation and stabilization of vortex rings in atomic Bose-Einstein condensates. We suggest an approach for generating vortex rings by optical tweezers—two blue-detuned optical beams forming a toroidal void in a magnetically or optically confined condensate cloud. We demonstrate that matter-wave vortex rings trapped within the void are energetically and dynamically stable. Our theoretical findings suggest a possibility for the generation, stabilization, and nondestructive manipulation of quantized vortex rings in experimentally feasible trapping configurations.

DOI: 10.1103/PhysRevA.88.043637 PACS number(s): 03.75.Kk, 05.30.Jp, 03.75.Lm, 67.85.−d

I. INTRODUCTION

A vortex ring is one of the most fascinating and universal structures in fluids of different nature. Well-known examples are smoke rings produced by smokers or an active volcano, bubble rings created by dolphins, and vortex rings in the blood stream produced by a human heart. Vortex rings have been the subject of numerous studies in classical fluid mechanics [1].

In quantum fluids and degenerate gases, vortex rings with a closed-loop core occupy a special place among other nonlinear excitations. Vortex rings play a crucial role in the decay of superflow and in quantum turbulence [2]. Several experimental schemes for creating vortex rings in atomic Bose-Einstein condensates (BECs) based on dynamical instabilities of collective excitations [3] or condensate collisions [4,5] have been successfully tested. Additional theoretical proposals involve the interference of two-component BECs [6], space-dependent Feshbach resonance [7], and phase imprinting methods [8].

In inhomogeneous trapped BECs, vortex rings turn out to be unstable (see, e.g., [6]), which substantially restricts their lifetimes and complicates experimental observation. A vortex ring either drifts to an edge of the condensate, where it decays into elementary excitations, or shrinks and annihilates within the condensate bulk.

In this paper, we propose an experimentally feasible trapping configuration that can be used to create, stabilize, and manipulate a vortex ring in a controllable and nondestructive manner. Our method for vortex-ring stabilization is based on a simple physical observation: when a superfluid flow involves fewer atoms, the energy cost to nucleate a vortex ring decreases because of a smaller contribution to the kinetic energy of the superfluid. Thus, the spatial position of the vortex core in a toroidal "antitrap" with the locally depressed atomic density is energetically preferable. In this paper, we propose to use repulsive blue-detuned laser beams to create a toroidal void in the bulk of the BEC cloud held in a large-scale magnetic or optical trap, which can be used to trap and guide a vortex ring. We demonstrate both energetic and dynamical stability of the vortex rings for realistic experimental parameters.

II. MODEL

Dynamical properties of ultracold dilute atomic BECs can be accurately described by the mean-field Gross-Pitaevskii (GP) equation

$$i\hbar\frac{\partial\tilde{\Psi}(\tilde{\mathbf{r}},t)}{\partial t}=\left[-\frac{\hbar^2}{2M}\Delta+\tilde{V}(\tilde{\mathbf{r}})+U_0|\tilde{\Psi}(\tilde{\mathbf{r}},t)|^2\right]\tilde{\Psi}(\tilde{\mathbf{r}},t), \quad (1)$$

where Δ is a Laplacian operator, $\tilde{V}$ is the trapping potential, $U_0=4\pi\hbar^2a_s/M$ characterizes the interaction strength, M is the mass of the atom, and a_s is the s-wave scattering length. The norm of the condensate wave function is equivalent to the number of atoms: $N=\int|\tilde{\Psi}|^2d\mathbf{r}$. Both the number of atoms and energy,

$$\tilde{E}=\int\left\{\frac{\hbar^2}{2M}|\nabla\tilde{\Psi}|^2+\tilde{V}(\tilde{\mathbf{r}})|\tilde{\Psi}|^2+\frac{U_0}{2}|\tilde{\Psi}|^4\right\}d\tilde{\mathbf{r}}, \quad (2)$$

are the integrals of motion of Eq. (1).

A vortex ring manifests itself in the emergence of a toroidal hole in the condensate, around which the atoms rotate poloidally with velocities $\tilde{\mathbf{v}}_s$ subject to the condition of quantized circulation (see, e.g., [9]): $Q\equiv\oint_\Gamma\tilde{\mathbf{v}}_s d\mathbf{l}=2\pi\hbar S/M$, where Γ indicates a closed contour around the vortex core and S is the integer topological charge of the vortex ring. The radius of the vortex core a_c is usually approximated by the healing length, $a_c\sim\tilde{\xi}=1/\sqrt{8\pi\tilde{n}a_s}$, where $\tilde{n}$ is the local condensate density in a zero-vorticity state.

The phase Φ of the BEC wave function $\tilde{\Psi}=|\tilde{\Psi}|e^{i\Phi}$ with the vortex ring is determined as follows: $\Phi(r,z)\approx S\theta$, where $r=\sqrt{x^2+y^2}$, which corresponds to the swirling superflow velocity $\tilde{\mathbf{v}}_s=(\hbar/M)\nabla\Phi\approx\mathbf{e}_\theta\hbar S/(Ml_z\rho)$, where ρ is the dimensionless distance from the ring core with the cylindrical coordinates (r_0,z_0), $\rho=\sqrt{(r-r_0)^2+(z-z_0)^2}$, and θ is the poloidal angle $\tan\theta(r,z)=(z-z_0)/(r-r_0)$ (see Fig. 1). In what follows, we use the characteristic scales of length $l_z=\sqrt{\hbar/(M\omega_z)}$ and time $\tau=\omega_z t$, where ω_z is the longitudinal trapping frequency. Dimensionless variables obtained using these scales are denoted by symbols without tilde: $E=\tilde{E}/(\hbar\omega_z)$, $\mathbf{r}=\tilde{\mathbf{r}}/l_z$, $\Psi=\tilde{\Psi}\sqrt{l_z^3}$, $n=|\tilde{\Psi}|^2l_z^3$, $\mathbf{v}_s=\tilde{\mathbf{v}}_s/(l_z\omega_z)$, etc.

In our model, the trapping potential is created by a large-scale spherically symmetric harmonic (e.g., magnetic) trap and two blue-detuned laser beams, namely, a radial Laguerre-Gaussian beam [10] and an elliptic highly anisotropic "sheet" beam, creating a tight repulsive potential in the z dimension.

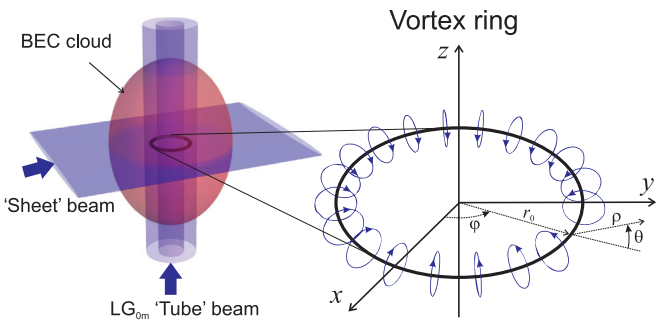

FIG. 1. (Color online) Left: Proposed trapping scheme for creation and manipulation of vortex rings. Right: Schematics of the condensate flow in a vortex ring. The circulation directions of the superflows swirling around the closed-loop core (black circle) are indicated by arrows.

The combined potential is given by

$$V = \tfrac{1}{2}(z^2 + r^2) + v_m(\beta r)^{2m} e^{-m[(\beta r)^2 - 1]} + v_z e^{-\alpha^2 z^2}, \quad (3)$$

where $\alpha = l_z/Z_{\rm T}$, $\beta = l_z/R_{\rm T}$, $Z_{\rm T}$ is the effective width of the sheet beam, $R_{\rm T}$ is the radial coordinate of the trap minima, and m is the topological charge of the red-detuned LG_{0m} optical beam. Here we consider single-charge ($S = 1$) vortex rings in a BEC cloud with $N = 10^6$ of ^{87}Rb atoms ($a_s = 5.77$ nm) in a harmonic trap with trapping frequency $\omega_z = 100$ Hz, and corresponding oscillator length $l_z = 5.88$ μm, and a tube beam with parameters $m = 1$, $\beta = 0.4$ ($R_{\rm T} = 6.57$ μm), and $v_m = 28$, unless specified otherwise.

In modeling nonequilibrium behavior, such as nucleation of vortex rings, dissipative effects are of crucial importance since they provide the mechanism for damping of elementary excitations in the process of relaxation to an equilibrium state. It is the dissipation that either causes the vortex core to drift to the BEC cloud edge (where vortex rings decay) or leads to the relaxation to the metastable state corresponding to the local minimum of the energy. Such effects naturally arise in a trapped condensate due to interaction with uncondensed atoms and can be captured phenomenologically by the dissipative GP equation derived by Choi *et al.* [11], in a manner similar to that originally proposed by Pitaevskii [12]. For a system close to thermodynamic equilibrium and subject to weak dissipation, the dissipative GP equation can be written in the form

$$i(1 + i\gamma)\frac{\partial \psi}{\partial \tau} = \left[-\frac{1}{2}\Delta + V(r,z) + g|\psi|^2 - \mu \right]\psi, \quad (4)$$

where we introduced the chemical potential of the equilibrium state, μ, as follows: $\Psi(\mathbf{r},\tau) = \psi(\mathbf{r},\tau)e^{-i\mu\tau}$, $-i\partial\psi/\partial t \approx \mu\psi$, and $g = 4\pi a_s/l_z$. The dissipative GP equation in the above form has been used extensively in previous studies of vortex dynamics [2,13,14].

The phenomenological damping rate $\gamma \ll 1$ depends on both the temperature and the spatial coordinates and can be approximately calculated using quantum kinetic theory [11]. In what follows, we neglect the position dependence of γ and set $\gamma = 0.03$ as in Ref. [2]; however, as we verified, our main results do not depend qualitatively on the specific value of $\gamma \ll 1$.

We assume that temperature of the condensate is well below the critical temperature for Bose condensation, $T < 0.5T_c$. In this regime, both the stochastic Gross-Pitaevskii equation, which properly accounts for classical noise due to thermal fluctuations, and the phenomenological dissipative GPE equation used here give similar results [15]. The noise produces a drift motion of collective excitations, such as dark solitons and vortices, and adds stochastic jitter to their trajectories [15]. However, the averaged dynamics of the collective excitations affected by weak classical noise is properly described by the dissipative GPE, as was demonstrated in [16].

Dynamical Eq. (4) with $\gamma > 0$ conserves neither the energy nor the number of particles. In our simulations, we adjust $\mu(\tau)$ on every time step so that the number of condensed particles slowly decays with time: $N(\tau) = N(0)e^{-\tau/\tau_0}$ to match the experimental measurements for atomic BECs. In our calculations we use the value of the parameter $\tau_0 = 10^3$, which corresponds to $t = 10$ s for the $1/e$ lifetime of the BEC reported in Ref. [17].

III. ENERGETIC AND DYNAMICAL STABILITY

To elucidate stability properties of a vortex ring in the trapping geometry described by Eq. (3), we discuss the energetic stability of the vortex rings in dissipationless condensate and then support our findings by numerical simulation of the dissipative GP equation (4).

In a homogeneous BEC, by the analogy with classical fluids and liquid helium, the energy of a large vortex ring can be estimated as follows (see, e.g., [18]): $E_n \approx 2\pi^2 S^2 n r_0[\ln(8r_0/a_c) - 1.615]$, r_0 is the radius of the ring, and a_c is the radius of the vortex core ($r_0 \gg a_c$). The Magnus force, which is directed outwards orthogonally to the ring velocity, stabilizes the ring against shrinking. As a result, in homogeneous condensate the ring travels with a constant speed $v_{\rm vr} \approx (S/r_0)[\ln(8r_0/a_c) - 0.615]$.

In a trapped, inhomogeneous BEC the vortex core undergoes precession around an *unstable* equilibrium position, corresponding to the maximum of the nucleation energy [6]. This is not surprising for a common axisymmetric trap. Indeed, the vortex energy depends on the product of the vortex ring radius r_0 and the local value of the density n, thus one might expect that the vortex nucleation energy decays both at the edge of the condensate, where density vanishes (close to the Thomas-Fermi surface), and when the vortex ring shrinks towards the axis of the trap where density is nearly constant. Certainly, the inhomogeneity of the condensate density must be properly accounted for in calculations of nucleation energy, but this correction, as we show below, does not change the main conclusions qualitatively.

Since the nucleation energy, $E_{\rm n} = E_{\rm v} - E_{\rm GS}$, is the energy difference for the state with imprinted vortex ring and the ground state, the main contribution to the nucleation $E_{\rm n}$ energy is given by the kinetic energy of the toroidal superflows

$$E_{\rm n} \approx \frac{1}{2}\int n\mathbf{v}_s^2 d\mathbf{r} = \frac{1}{2}S^2 \int n\rho^{-2} d\mathbf{r}.$$

Let us calculate the vortex ring energy, accounting for the condensate inhomogeneity caused by the trapping potential and toroidal hole around the vortex core. First, using the imaginary time propagation method, we find numerically the ground state $\psi_{GS}(r,z)$ of a BEC in the given trapping potential. Then we imprint the offset vortex ring core onto the ground state:

$$\Psi(r,z) = A[f(r,z)]^S \psi_{GS}(r,z) e^{iS\theta}, \tag{5}$$

where A is the constant of normalization introduced to preserve the number of atoms, the function $f(r,z) = \tanh(\rho/\xi)$ interpolates the order parameter Ψ properly both in the vicinity of the core, $\Psi \sim \rho^S$ if $\rho \to 0$, and well away from the core, $|\Psi| \sim |\psi_{GS}|$ if $\rho \gg \xi$. Using the ansatz (5) we obtain the nucleation energy as the function of the vortex core coordinate. The pronounced minimum of E_n in the vicinity of the minimum of the condensate density is clearly seen from Fig 2(a), where the nucleation energies per particle are shown for different values of the tube-beam intensities v_m.

We have verified our energetic stability analysis by extensive numerical simulations of the dissipative GP equation (4) with the split-step Fourier transform method. Nonstationary initial conditions obtained by imprinting the offset vortex ring core onto the ground state were used. By changing the initial position of the vortex core we have found remarkable agreement between the results of direct numerical simulations and predictions based on the energetic stability analysis. The typical examples of the vortex ring evolution are presented in the Supplemental Material [19].

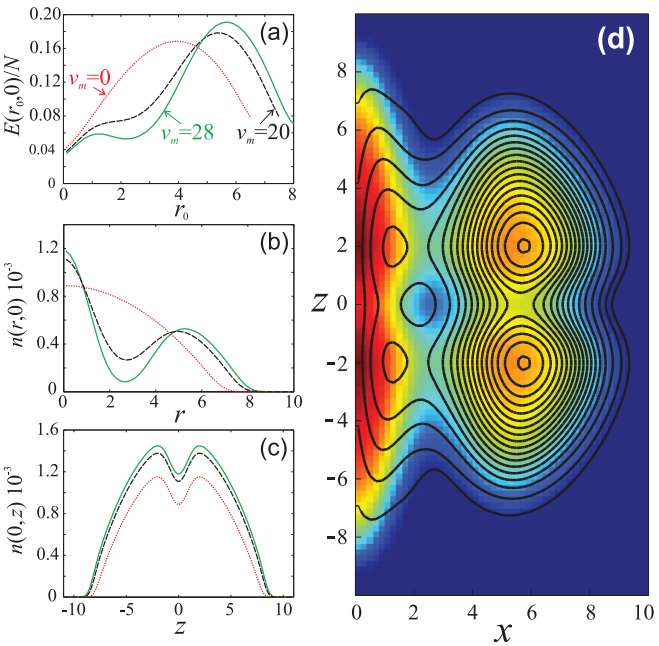

FIG. 2. (Color online) (a) Nucleation energy of the vortex ring per particle $E(r_0,0)/N$ for different values of the tube-beam intensity. The values of v_m are indicated near the curves; other parameters are $v_z = 10$, $\alpha = 0.8$, $\beta = 0.4$, and $N = 10^6$. Density profiles $|\psi|^2 \times 10^{-3}$ of the condensate in the ground state for the same values of v_m: (b) the radial part of the density profile at $z = 0$; (c) the longitudinal distribution of the density at $r = 0$. (d) Distribution of $|\psi(x,0,z)|$ with contour lines for nucleation energy.

As noted above, the thermal fluctuations are not accounted for in our model since the BEC temperature is assumed to be well below T_c. The noise associated with thermal fluctuations would convert the smooth trajectory of the vortex core into a Brownian-like motion [15]; however, the resulting averaged direction of the vortex ring drift towards the lower density region is still well described by our model. Once the local energy minimum is reached and the vortex ring is relaxed into the metastable state, any noise would only cause stochastic oscillations in the vicinity of the local equilibrium position. On the other hand, the number of condensed atoms continues to decrease with time, thus the depths of the potential well for the vortex rings becomes weaker. For the substantially depleted condensate, even small stochastic perturbations could in principle considerably restrict the lifetime of the vortex rings. Therefore, the detailed analysis of the influence of thermal fluctuations on the vortex rings in BECs deserves further investigation.

IV. GENERATION OF VORTEX RINGS

Having established energetic and dynamical stability of vortex rings in the toroidal void created by the trapping potential (3), we now analyze two methods for their nucleation, trapping, and stabilization. The first method employs interference between BECs loaded in a large-scale harmonic potential and separated by a potential barrier. A similar method was used in theoretical [14] and experimental investigations [5] of the vortex ring generation, where a tight (in the z direction) barrier rapidly vanished, with the resulting interference between two identical condensates giving rise to pairs of the vortex-antivortex rings. Here we use the barrier that initially separates the condensate into two unequal parts, and then is lowered nonadiabatically rather than being completely removed. The interaction through the finite barrier ensures that the coherence within the cloud is retained. A typical example of subsequent evolution displaying generation and trapping of the vortex rings is shown in Fig. 3. As soon as the barrier becomes sufficiently low, both the repulsive interatomic interaction and the magnetic trapping potential propel the atoms from the upper half of the condensate to fill in the appearing emptiness. The various vortex rings are generated during collision of the upper half of the BEC cloud with the sheet beam and the rest of the condensate. The cores of the vortex rings are indicated by crosses; antivortex rings are marked by circles in Fig. 3.

Note that one of the nucleated vortex rings appears outside the Thomas-Fermi surface of the condensate, then it shrinks and enters the BEC cloud at the depth corresponding to its energy and moves close to the surface of constant energy until it reaches the toroidal void [see Fig. 3(d)]. Finally it relaxes to the stable state, as seen in Fig. 4. Thus the single vortex ring, born on the periphery, drifts to the stable position, where it is caught in the toroidal void.

The second method is designed to stabilize the vortex-antivortex pair inside the condensate. The *red-detuned* laser beam creates additional attractive potential $-|v_z^{(r)}(\tau)| \exp(-\alpha_r^2 z^2)$ with the maximum intensity at $z = 0$ and $\alpha_r = 2$. Starting from zero value, the intensity of the red-detuned beam ramps up linearly with time so that at $\tau_z = 0.1$ it reaches the value $|v_z^{(r)}(\tau_z)| = v_z = 20$ and remains

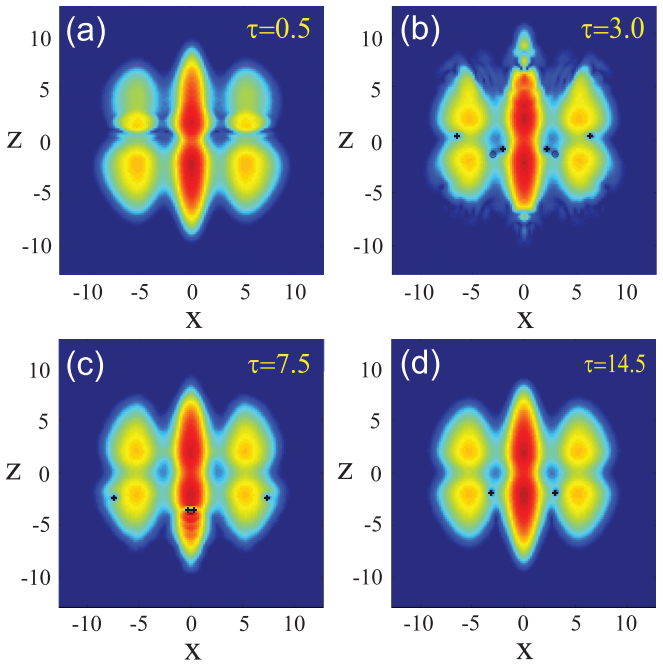

FIG. 3. (Color online) Typical example of vortex ring generation and further stabilization. The snapshots of the cross section $|\psi(x,0,z)|$ are shown for different moments of time. Parameters of the sheet beam change from $\alpha = 0.4$, $v_z = 20$ and centered at $z = 0.5$ to $\alpha = 0.8$, $v_z = 10$ and centered at $z = 0$.

unchanged during further evolution. The growing attractive potential draws in the condensed atoms and creates supercritical counterflows directed to the $z = 0$ plane. Conservation of circulation ensures that vortex rings and antivortex rings are nucleated simultaneously (see Fig. 5). Some of the vortex rings move out and decay at the cloud's edge, but one vortex-antivortex pair relaxes to the stationary state, so that each ring is stored in its own toroidal void, separated by the local density maximum at $z = 0$. It should be emphasized that the vortex rings are generated in the low-density regions, where the

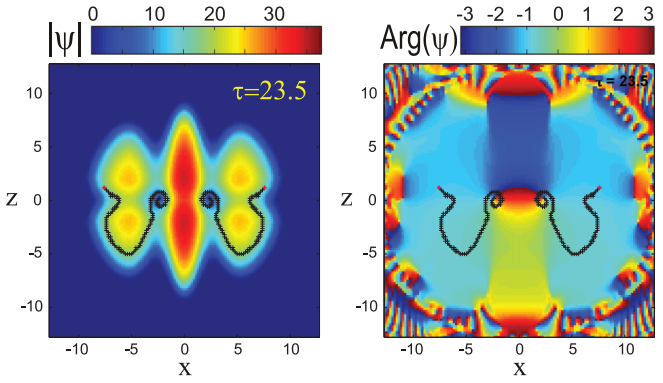

FIG. 4. (Color online) Trapped and stabilized vortex ring as the result of vortex ring nucleation presented in Fig. 3. Shown are $|\psi|$ (left) and phase (right) of the order parameter at $\tau = 23.5$. The subsequent positions of the vortex core of the stable vortex ring are marked by the sequence of black crosses. The red dots close to the condensate edge indicate the position where the nucleated vortex ring was first detected.

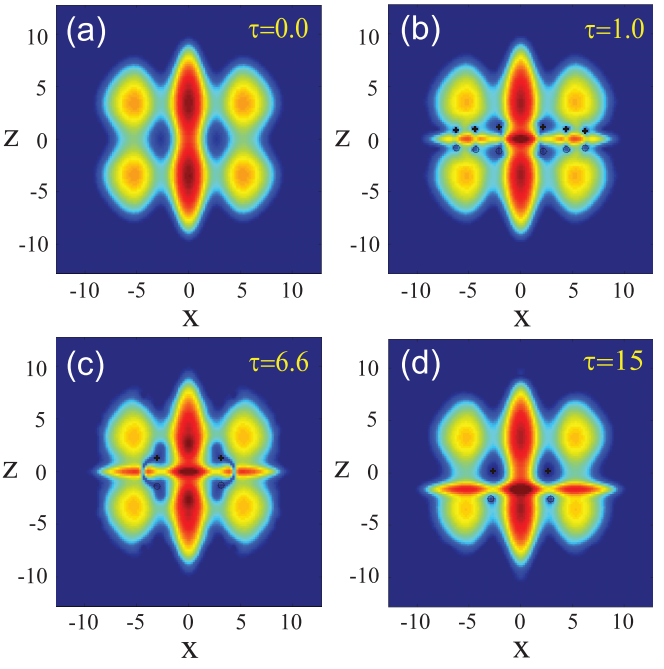

FIG. 5. (Color online) Generation and stabilization of the vortex-antivortex rings. (a) Initial condition is the BEC divided in half by a wide blue-detuned repulsive sheet beam with $\alpha = 0.4$, $v_z = 20$; (b) three vortex-antivortex pairs are seen. The cores of the vortex rings are indicated by crosses, antivortex rings are marked by circles. (c) Vortex-antivortex pair relaxes to the stationary state; (d) the antivortex ring is detached by the moving red-detuned beam in a controllable way.

critical velocity is reached first. Obviously, the toroidal voids are the most preferable places for vortex ring nucleation, that is why in these regions the superflow readily decays generating the vortex rings. Thus, the generation and stabilization of the vortex-antivortex pairs unfailingly accompany the decay of the counterflowing superflows in the considered geometry of the trapping potential.

As soon as the pair of vortex rings is stabilized, we start slowly shifting down the red-detuned sheet beam. When this beam enters and eliminates the lower toroidal void, the antivortex ring becomes untrapped [see Fig. 5(d)]. The decoupled antivortex ring starts moving to the edge of the cloud and finally decays into elementary excitations. We note that these excitations could be detected in the experiment. Detection of the outbursts of the excitations at well-defined moments of time could be used as the decisive evidence that the vortex ring is generated and stabilized successfully. The velocity of the sheet beam, $v_b = 0.5$, is chosen to be well below the critical velocity (see, e.g., Refs. [20,21]), so that new vortex rings appear and decay only in the low-density periphery, i.e., only when the red-detuned beam nearly completely leaves the BEC cloud. After some relaxation time the remaining single vortex ring occupies the stable position.

The combination of optical trapping and antitrapping potentials created by the optical beams represents a kind of *optical tweezers* for manipulation of vortex rings; the vortex ring can be "picked up", stabilized, and then moved to a new location by gradually adjusting the parameters of the optical trap. We note that the method for the vortex ring

stabilization proposed here can, in principle, be realized in existing experimental setups (see, e.g., Ref. [17]).

V. CONCLUSIONS

We have proposed an approach for the generation and stabilization of vortex rings in toroidal optical tweezers. We have proved that the nucleation energy of a vortex ring as the function of the vortex core position has a pronounced minimum within the toroidal void. Strictly speaking, this means that the vortex rings are metastable. In practice, a dissipation of the vortex energy is universally present. As a result, the vortex ring trapped in the region with locally reduced density relaxes to the stationary state with the radius corresponding to a local minimum of the nucleation energy. Although here we considered a BEC well below the condensation temperature, so that the dynamics of the vortex rings is only weakly affected by thermal noise, the influence of the condensate depletion and thermal fluctuations on the stability of the vortex rings merits a separate study.

Our findings not only suggest the possibility for experimental demonstration of the stable vortex rings, but also offer an approach for nondestructive manipulation of vortex rings. We hope that the described method will help to elucidate the properties of vortex rings in superfluid media, which is a problem of fundamental interest.

ACKNOWLEDGMENTS

The authors thank N. Berloff and C. Conti for useful discussions. The work was partially supported by the Australian Research Council.

[1] P. G. Saffman, *Vortex Dynamics* (Cambridge University, Cambridge, England, 1992).
[2] M. Tsubota, M. Kobayashi, and H. Takeuchi, Phys. Rep. **522**, 191 (2013).
[3] B. P. Anderson, P. C. Haljan, C. A. Regal, D. L. Feder, L. A. Collins, C. W. Clark, and E. A. Cornell, Phys. Rev. Lett. **86**, 2926 (2001).
[4] N. S. Ginsberg, J. Brand, and L. V. Hau, Phys. Rev. Lett. **94**, 040403 (2005).
[5] I. Shomroni, E. Lahoud, S. Levy, and J. Steinhauer, Nat. Phys. **5**, 193 (2009).
[6] B. Jackson, J. F. McCann, and C. S. Adams, Phys. Rev. A **61**, 013604 (1999).
[7] F. Pinsker, N. G. Berloff, and V. M. Pérez-García, Phys. Rev. A **87**, 053624 (2013).
[8] J. Ruostekoski and J. R. Anglin, Phys. Rev. Lett. **86**, 3934 (2001).
[9] C.-H. Hsueh, S.-C. Gou, T.-L. Horng, and Y.-M. Kao, J. Phys. B **40**, 4561 (2007).
[10] E. M. Wright, J. Arlt, and K. Dholakia, Phys. Rev. A **63**, 013608 (2000).
[11] S. Choi, S. A. Morgan, and K. Burnett, Phys. Rev. A **57**, 4057 (1998).
[12] L. Pitaevskii, Sov. Phys. JETP **8**, 88 (1959).
[13] K. Kasamatsu, M. Tsubota, and M. Ueda, Phys. Rev. A **67**, 033610 (2003).
[14] R. Carretero-González, N. Whitaker, P. G. Kevrekidis, and D. J. Frantzeskakis, Phys. Rev. A **77**, 023605 (2008).
[15] S. J. Rooney, A. S. Bradley, and P. B. Blakie, Phys. Rev. A **81**, 023630 (2010).
[16] S. P. Cockburn, H. E. Nistazakis, T. P. Horikis, P. G. Kevrekidis, N. P. Proukakis, and D. J. Frantzeskakis, Phys. Rev. Lett. **104**, 174101 (2010).
[17] A. L. Gaunt, T. F. Schmidutz, I. Gotlibovych, R. P. Smith, and Z. Hadzibabic, Phys. Rev. Lett. **110**, 200406 (2013).
[18] C. F. Barenghi and R. J. Donnelly, Fluid Dynam. Res. **41**, 051401 (2009).
[19] See Supplemental Material at http://link.aps.org/supplemental/10.1103/PhysRevA.88.043637 for the typical examples of the vortex ring evolution.
[20] C. Raman, M. Köhl, R. Onofrio, D. S. Durfee, C. E. Kuklewicz, Z. Hadzibabic, and W. Ketterle, Phys. Rev. Lett. **83**, 2502 (1999).
[21] P. Engels and C. Atherton, Phys. Rev. Lett. **99**, 160405 (2007).